Oceanic rainfall observation using passive acoustic method

BARRY B. MA Ph.D.

Assistant Professor
Marine Science Department
Naval Academy
Kaohsiung, Taiwan

ABSTRACT

Rainfall measurement over the ocean is very difficult to achieve because of its inhomogeneity in both time and space. The natural roughness of air-sea interface produces a potentially catastrophic environment for surface instruments on moorings, and this is reflected in the data quality from physical collection-types of rain gauges on moorings. Other techniques for measuring the rainfall over the ocean use satellite- based instruments. These should provide a large-scale coverage for the measuring different parameters associated with rainfall. However, the satellite's temporal resolution is usually very low, and the surface truth is also needed for the calibration purpose. An alternate technique for measuring the oceanic rainfall is using the underwater sound. The technique of passive monitoring of the ocean rainfall using ambient sound depends on the accuracy of sound pressure level (SPL) detection. The underwater Passive Acoustic Listeners (PALs) were developed for this purpose. Over 90 buoy-months of ambient sound spectra have been collected on the Tropical Atmosphere Ocean Project (TAO) array since 1998. The probability of rain-event detection rate is 100% when the rainfall rate is higher than 15 mm/hr with false alarm rate at minimal 0.4 %. The rainfall parameters derived from an acoustic discrimination process are compared with a satellite based product, the Tropical Rain Measuring Mission (TRMM) 3B42. The acoustic rainfall accumulations show the comparable results in both long (year) and short (hours) time scales.

1. Introduction

The ocean ambient noise has long been noted as presenting an "unwanted" background sound at any given location and time. Different sources of ambient sound contribute to the overall sound level at different frequency ranges and time spans. Some of the sources are also heavily depend on the location. For example, at some continental shelf regions, biological sounds related to a particular fish could be the dominant ambient noise source. Sites near ocean shipping lanes are much noisier than other open ocean locations at the low frequencies. For the higher frequencies (50 kHz plus), thermal noise is a dominant source whereas the other sources are often attenuated.

For the frequency range from 1 to 50 kHz, wind generated noise is the major persistent noise source component, characterized by a spectrum with a uniform negative slope. However when rain is present, the rain generated sound usually dominates all the other sources in this frequency band. In summary, the ocean ambient sound is time, frequency, and location dependent. If one can detect when a particular dominant source is present (e.g. rain), then that "unwanted noise" can be treated as a "wanted signal" and be used to quantify its presence. The temporal and frequency distribution of typical sources of ocean ambient sound are illustrated in Fig. 1. Rainfall measurement over the ocean is very difficult to achieve because of its inhomogeneity in both time and space. Furthermore, the natural roughness of air-sea interface produces a potentially catastrophic environment for surface instruments on moorings, and this is reflected in the data quality from physical collection-types of rain gauges on moorings. Other techniques for measuring the rainfall over the ocean use satellite- based instruments. These should provide a large-scale coverage for the measuring different parameters associated with rainfall. However, the satellite's temporal resolution is usually very low (e.g. eight satellite passes per day). In addition, surface truth measurements are needed for rainfall. Luckily, rain is also one of the principal natural sources of underwater sound (Nystuen 2000). This allows acoustic measurements of rainfall. Although there are sometimes man-made or biological noises that are loud and could potentially interfere with the acoustical measurement of rain, these noises are generally intermittent or geographically localized.

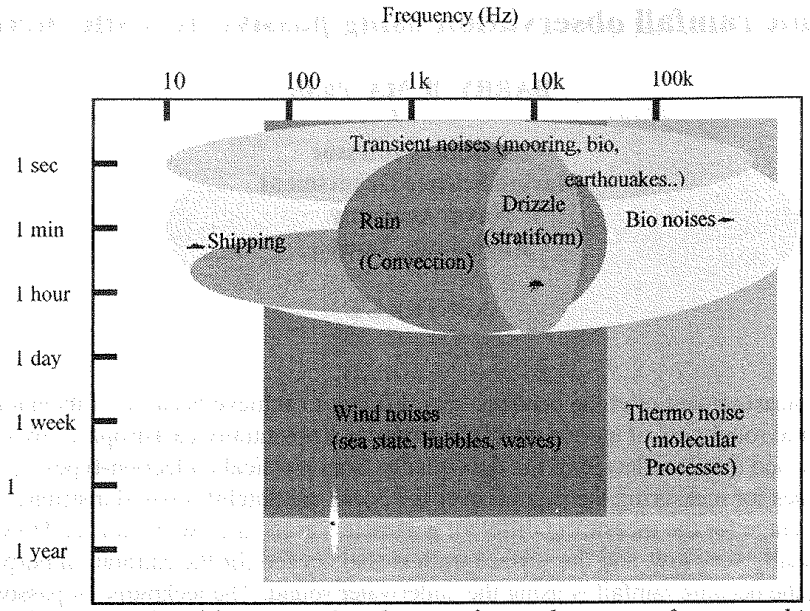

Fig. 1. The temporal and frequency distribution of typical sources of ocean ambient sound.

2. Background

Naturally occurring raindrops range in size from about 300 microns diameter (a drizzle droplet) to over 5 mm diameter (often at the beginning of a heavy downpour). As the drop size changes, the shape of the splash changes and so do the subsequent sound production. Laboratory and field studies (Medwin et al., 1992; Nystuen 1996, 2001) had been used to identify five acoustic raindrop sizes (Table 1). For tiny drops (diameter < 0.8 mm), the splash is gentle, and no sound is detected. On the other hand, small raindrops (0.8 - 1.2 mm diameter) are remarkably loud. The impact component of their splash is quiet, but the geometry of the splash is such that a bubble is generated by every splash in a very predictable manner (Pumphrey et al. 1989). These bubbles are relatively uniform in size, and therefore frequency, and are very loud underwater. Small raindrops are present in almost all types of rainfall, including light drizzle, and are therefore responsible for the remarkably loud and unique underwater "sound of drizzle" heard between 13-25 kHz, the resonance frequency for these bubbles. Interestingly, the splash of the next larger raindrop size, medium (1.2-2.0 mm diameter), does not trap bubbles underwater, and consequently medium raindrops are relatively quiet, much quieter than the small raindrops. The only acoustic signal from these drops is a weak impact sound spread over a wide frequency band. For large (2.0-3.5 mm diameter) and very large (> 3.5 mm) raindrops, the splash becomes energetic enough that a wide range of bubble sizes are trapped underwater during the splash, producing a loud sound that includes relatively low frequencies (1-10 kHz) from the larger bubbles. For very large raindrops, the splat of the impact is also very loud with the sound spread over a wide frequency range (1-50 kHz). Thus, each drop size produces sound underwater with unique spectral features that can be used to acoustically identify the present of that drop size within the rain.

Table 1. Acoustic raindrop sizes. The raindrop sizes are identified by different physical mechanisms associated with the drop splashes (Nystuen 2001).

Drop Size	Diameter	Sound	Frequency range (kHz)	Splash character
Tiny	< 0.8 mm	Silent		Gentle
Small	0.8-1.2 mm	Loud bubble	13 - 25	Gentle with bubble every splash
Medium	1.2-2.0 mm	Weak impact	1 - 30	Gentle, no bubbles
Large	2.0-3.5 mm	Impact, Loud bubbles	1 - 35 2 - 35	Turbulent Irregular bubble entrainment
Vary Large	>3.5 mm	Loud impact Loud bubbles	1 - 50 1 - 50	Turbulent Irregular bubble entrainment Penetrating jet

In any given time, the local hydrophone pressure at the measurement site can be expressed as the sum of all sound sources around the hydrophone in micropascals,

$$P_a = P_r + P_w + P_{ss} + P_{ml} + P_{st} + P_{other} \quad (1)$$

where *r, w, ss, ml,* and *st* denote rain, wind, sea state, marine life and ship traffic respectively (Black et al, 1997). The SPL in decibels (dB) can be expressed as

$$SPL(f) = 10\log_{10}\left(\frac{P_a^2}{P_{ref}^2}\right) \qquad dB\ re\ 1\mu Pa^2/Hz \quad (2)$$

where P_a^2 is the variance of the pressure fluctuations in the 1 Hz bandwidth, and P_{ref} is the reference level at 1

μPa^2 /Hz. The contribution to the pressure fluctuation from different sources cannot be separated since they are indistinguishable. But if different sources have unique frequency spectrum *SPL(f)*, then times with only particular sources present can be identified, for example, P_w (wind only), P_r (rain only), and $P_r + P_w$ (rain and wind combined).

The pressure signal due to wind and rain comes from the ocean surface. If the sound source is assumed to be uniformly distributed, then the sound intensity at source depth, *h*, below the surface can be related to the sound intensity at the surface, I_0 by

$$I(h) = \int I_0 \cos^2\theta \quad atten(p)\, dA \qquad (3)$$

where θ is the zenith angle and *atten(p)* describes the attenuation due to geometric spreading and absorption along the acoustic path, *p*. By relating I_0 to rainfall rate, acoustic measurements at rainfall rate can be obtained (Nystuen, 2001). If absorption and refraction are neglected, the measurement should be independent of depth. For any particular deployment, the attenuation along the acoustic path can be complicated, but have only resulted in minor corrections in other studies (Vagle et al. 1990).

3. The instrument - Acoustic Rain Gauges (ARGs)

The Acoustic Rain Gauges (ARGs) consist of an ITC-8263 hydrophone, signal pre-amplifiers and a recording computer (Tattletale-8) (Fig. 2).

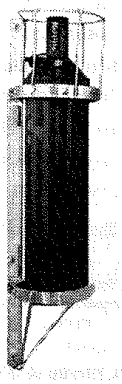

Fig. 2. Acoustic Rain Gauge

The nominal sensitivity of these instruments is -160 dB relative to 1 V/μPa and the equivalent oceanic background noise level of the pre-amplifier system is about 28 dB relative to 1 μPa^2/Hz. Band-pass filters are present to reduce saturation from low frequency sound (high pass at 300 Hz) and aliasing from above 50 kHz (low pass at 40 kHz). The ITC-8263 hydrophone sensitivity also rolls off above its resonance frequency, about 40 kHz. A data collection sequence consists of four 1024 point time series collected at 100 kHz (10.24 ms each) separated by 5 seconds if triggered by rain or drizzle. Each time series is fast Fourier transformed (FFT) to obtain a 512-point (0-50 kHz) power spectrum. These four spectra are averaged together and spectrally compressed to 64 frequency bins, with frequency resolution of 200 Hz from 100-3,000 Hz and 1 kHz from 3-50 kHz. These spectra are evaluated individually to detect the acoustic signature of rainfall and then are recorded internally.

The ARGs have been deployed on the Tropical Atmosphere Ocean project (TAO) moorings since 1998 at different locations with depths from 28 to 98 meters. The depth was chosen to be above the thermocline, lessening the effects of acoustic refraction, and to maximize sampling area, so that the buoy itself does not occupy a significant portion of the effective listening area. Eqn. 3 can be used to estimate the effective sampling area at the surface. Neglecting refraction and absorption, 90% of the signal is arriving from a sampling area equal to:

$$\text{Surface sampling area} \cong \pi(3h)^2 \qquad (4)$$

where *h* is the depth of the hydrophone. The integrating area of the hydrophone is important for two reasons. First, rainfall is inhomogeneous on all scales, but rainfall measurements are needed on large temporal or spatial scales. An instrument with a large inherent sampling area should produce a better "mean" rainfall statistic. Second, the large spatial sampling allows the short temporal sampling periods being used for each data sample to include many individual raindrop splashes (Nystuen 2001).

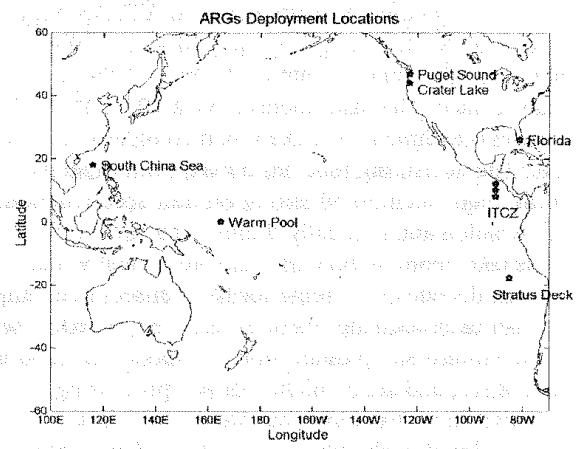

Fig. 3. The deployment of ARGs in different climate regions since 1996. The data at the Pacific warm pool and Intertropical Convergence Zone (ITCZ), which have about 90 buoy-months acoustic record are used in this study.

The signal contains sound from the desired geophysical quantity, plus sounds from wind and noises from other sources. Two climate regions, the Pacific warm pool and Inter-tropical Convergence Zone (ITCZ), have been chosen for this study. These open ocean locations have less contribution from bottom reverberation and biological sources than continental shelf regions. About 90 buoy months of acoustic data are available for our analysis. ARGs have also been deployed in several different climate regions as shown in Fig. 3.

4. Ancillary data from mooring and satellite

Pacific Marine Environmental Laboratory (PMEL) moorings data and Tropical Rain Measuring Mission (TRMM) satellite data are used in the intercomparison of ARGs data for algorithm development and validation.

a. Data from ATLAS mooring

The Next Generation Autonomous Temperature Line Acquisition System (ATLAS) buoys (Milburn et al. 1996) are deployed throughout the tropical Pacific and Atlantic Oceans. The ARGs were mounted on the mooring lines at the various locations. Selected ancillary data sets from the moorings are used in our study.

1) R.M. YOUNG ANEMOMETER DATA

The R.M. Young Company anemometer is mounted on the ATLAS mooring at 4 meters height. The data values are 10-minute averaged wind vectors. The error estimate is ±0.3 m/s or 3% of the wind speed, whichever is greater (Freitag et al 2001). By using the Coupled Ocean-Atmosphere Response Experiment (COARE) V2.5 flux algorithm (Fairall et al. 1996), these values are converted to equivalent 10 meters height wind speed.

2) R.M. YOUNG RAIN GAUGES DATA

Precipitation measurements on ATLAS buoys are made using R.M. Young Company Model 50203-34 self-siphoning rain gauges mounted 3.5 meters above the ocean surface. The instruments have a 100-cm^2 (11.3-cm diameter) catchment cylinder mounted on top of a fill tube. The measuring tube has a maximum capacity of 500mL, equivalent to 50 mm of rainfall accumulation, after which it automatically drains via a siphon. Siphon events take about 30 seconds, and are typically identified by sharp declines in volume for two consecutive samples. In real-time processing, these events are ignored. The 1-minute volume samples are stored on board the mooring while at sea, and are available for postprocessing after recovery. In post-deployment processing, data associated with siphon events are flagged, typically removing three minutes worth of data centered on the event. Once the mooring is recovered, the 1-minute accumulations are first flagged for obviously erroneous data. A 16-min Hanning filter is then applied to these data to generate smoothed 10-minute accumulations. The estimated instrumental error for 10-minute derived rainfall rates is 0.4 mm/hr when the rain present, and is 0.1 mm/hr when there is no rain (Serra et al. 2001).

b. TRMM precipitation product 3B42

The Tropical Rain Measuring Mission (TRMM) is a satellite dedicated to the measurement of precipitation in the tropics. TRMM satellite was launched on November 27, 1997 and is maintained an altitude approximately 350 km and an inclination of 35 degrees to the Equator. The satellite acquires approximately 16 orbits of data per day for mapping tropical rainfall between latitudes of 38 degrees north and south of the equator. Rainfall sensors include a precipitation radar (PR), a microwave imager (TMI) and a visible/infrared sensor (VIRS). Data from these instruments are combined in a variety of ways to produce rainfall products which are available through the NASA Goddard Distributed Active Archive Center (DAAC). Several levels of process are used in producing different products. The rainfall product 3B42 is a daily precipitation product which produced from spatially averaged on a 1° by 1° grid which combined rain structure (2B31) and VIRS calibration (1B01) to adjust IR estimates from geosynchronous IR observations. Global estimates are made by adjusting the GEOS Precipitation Index (GPI) to the TRMM estimates.

5. Evaluation of acoustic discrimination process in rainfall

The acoustic data are processed through a series of discrimination process (Ma and Nystuen, 2005). To evaluate the success of the acoustic discrimination process, a simple optimal decision matrix, the binary decision statistic (Urick, 1983) is adopted (Fig. 4). The input data are the R. M. Young surface rainfall rates for 10-minute intervals, and with a "positive" detection threshold set at 0.4 mm/hr. The ARG rain detection is set as the output decision. Correct detection, missed detection, and false alarm categories are further binned into rainfall rates with bin width 5mm/hr (Fig. 5). Three different process stages: 1) initial screening (solid line), 2) noise removal (dotted line), and 3) continuity check (dashed line), are shown in this evaluation. Initially the false alarm rate is very high. After the discrimination process the false alarm rate became acceptable. The trade-off to this reduction in false alarm is the shift of "correct decisions" to "missed detections". However for rainfall rates higher than 15 mm/hr, the discrimination process does not shift any correct decisions to missed detections, while the false alarm rate drops to nearly zero.

Rainfall rate (mm/hr) Every 10 minutes		Decision (ARGs spectra)	
		Rain	No-Rain
Input RMY R: Rainfall rate (mm/hr)	Rain	**Correct** Pd(R) Criteria: RMY ≥ 0.4 mm/hr; ARG detected at least one precipitation spectra.	Missed Pm(R) Criteria: RMY ≥ 0.4 mm/hr; No ARG detection at all.
	No-Rain	**False Alarm** Criteria: RMY < 0.4 mm/hr. ARG detected at least one precipitation spectrum.	**Correct** (Null decision) Criteria: RMY < 0.4mm/hr; No ARG detection at all

Fig. 4. The binary optimal decision matrix scheme. The input is RMY self-siphoning rain gauge 10-minute rainfall. The output decision is the ARG precipitation detection.

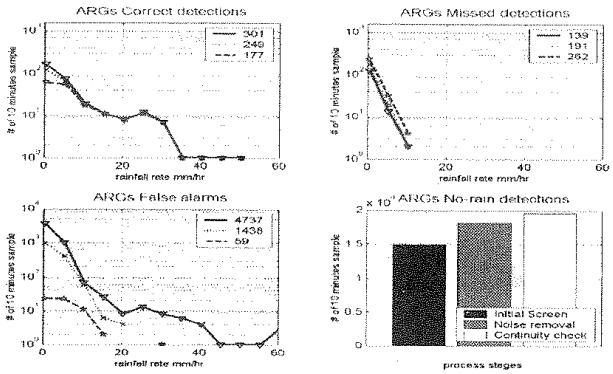

Fig. 5. Optimal decision matrix of detection in different discrimination process stages. The solid line is the initial screening. The dotted line is after Noise removal but before the continuity check, and the dashed line is the final product after the continuity check. The number in the legend boxes represents overall number of samples in each category. The data are separated into 5mm/hr bin width. The rainfall rate used for the "correct" and "missed" detection categories are from the R.M. Young surface rain gauge, while the rainfall rate for the "false alarm" category is from the ARG data.

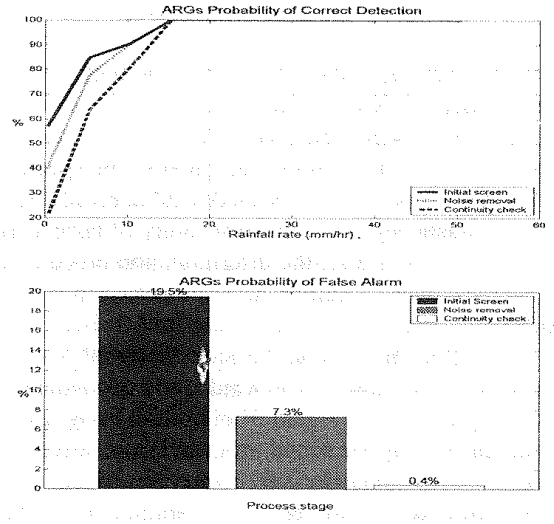

Fig. 6. The probability of correct detection is calculated from the "correct" and "miss" categories in the binary decision matrix. The probability of false alarm is calculated from the "false alarm" and "null decision" categories.

The probability of detection is calculated from the ratio of correct to "missed" detection. The probability of detection is increased as the rainfall rate increases and reaches 100 % when the rainfall rate is over 15 mm/hr (Fig. 6). The probability of false alarms is calculated from the ratio of false alarm and null decision (no rain in both instruments). Through the discrimination process, the probability of false alarm is reduced from 19.5 % to 7.3 % (after noise removal) to the final 0.4 % (after continuity check). The discrimination process has eliminated most of the false alarms and still maintained a high probability of detection, at least for rainfall rate over 5mm/hr. The sources of errors in this analysis will be the detection errors from both instruments since the true rainfall is unknown and errors are possible for both instruments.

6. Rainfall quantification - empirical algorithm for deep open-ocean

A simple relationship between sound intensity and rainfall rate (mm/hr) can be written in the form of

$$I = aR^b \qquad (5)$$

where I is the sound intensity and R is the rainfall rate. Taking $10\log_{10}$ of Eqn. 5 at 5 kHz, this becomes

$$dBR/10 = (SPL_{5kHz} - a')/b' \qquad (6)$$

where $dBR = 10\log_{10}(R)$, a' represents the intercept and b' is the slope. The acoustic rainfall signal at 5 kHz is chosen because it has a large dynamic range and is in a part of the acoustic spectrum not thought to be affected by wind speed (Nystuen, 2001). Similar empirical algorithm of rainfall rate conversion was proposed by Nystuen (1996) based on observations from a shallow brackish pond near Miami, FL:

$$dBR/10 = (SPL_{5kHz} - 50)/17 \qquad (7)$$

where R is the rainfall rate in mm/hr. Using the R. M. Young data as a guide for rainfall rate and the acoustic sound pressure level (dB) at 5 kHz, a new empirical algorithm for rainfall rate versus sound pressure level can be produced. The new result suggests an algorithm for those data sets of

$$dBR/10 = (SPL_{5kHz} - 42.4)/15.4 \qquad (8)$$

The standard deviation for the difference between ARG estimate rainfall rate using Eqn. 8 and R. M. Young rainfall rate is in the order of 0.25. It's quite large and most likely due to the sampling area covered and nature variability of rainfall. This algorithm is also quite different from the previous study. In particular, the sound level reported from the open ocean locations appears to be nearly 10 dB quieter than in the Miami, FL data. Presumably, the bottom reverberation of the shallow fresh water pond versus the deep open ocean condition is responsible for the changes in the empirical algorithm.

7. Validation of rainfall rate algorithm

Rainfall accumulations for the Year 2001 at the 10° N, 95°W and 12 °N, 95°W TAO moorings are shown in Fig. 7. The acoustic rainfall accumulation is calculated by applying the rainfall rate algorithm (Eqn. 8) and is compared with the co-located R.M. Young rain gauge and TRMM satellite rainfall product 3B42. This part of the ocean has a distinctive rainy season beginning in May and lasting into October. Exact agreement between the satellite estimate and the surface instruments should not be expected, since the sampling strategies are very different (spatial averaging versus high temporal resolution). However, seasonal agreement should be expected. The comparison shows that the R.M. Young gauge and ARG at the 10°N, 95°W has excellent agreement for both individual events and for the annual

accumulation (Fig. 7 top). At 12°N, 95°W, the R.M. Young gauge did not function properly during several time periods (Fig. 7 bottom). The accumulation measurement of R.M. Young data is shifted to match the ARG accumulation after each period of non-performance. The R.M. Young and ARGs are in good agreement when both instruments were functioning properly. The ARGs also has very good seasonal agreement with TRMM. The difference in annual rainfall estimate is less than 5 %. The scatter plots for daily accumulation are shown in Fig. 8. The ARGs and R.M. Young shows very good agreement (Fig. 8 top), but the ARGs and TRMM (Fig. 8 bottom) shows the satellite measurement does not have any daily rainfall accumulation over 50mm. This probably reflects the spatial sampling limitations of satellite rainfall estimation compared to the more localized acoustic measurement of rainfall.

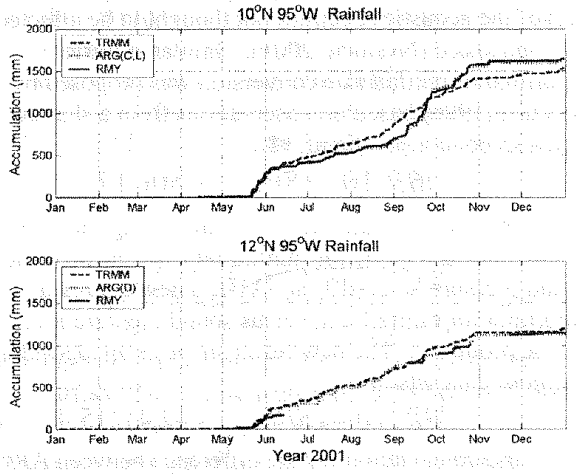

Fig. 7. The rainfall accumulation in 10° and 12°N, 95°W in 2001. The dotted line is the ARGs, solid line is R. M. Young, and dash line is TRMM rainfall accumulation (mm). On the top panel, the ARGs and R.M. Young has excellent agreement in both rainfall events and overall accumulation. The TRMM data also shows general seasonal agreement. On the bottom panel, the R.M. Young data was missing in some periods during the deployment. The accumulation of R.M. Young has been offset by applying the acoustic rainfall conversion data. The difference in annual rainfall estimate is less than 5 %.

8. Conclusions

The rainfall measurement over the ocean using ambient sound relies on the accuracy of sound pressure level measurement. An empirical rainfall conversion algorithm based on a single frequency (5 kHz) is proposed and tested on the year long deployment at 10°N, 95°W and 12°N, 95°W in 2001. The results show the excellent agreement in both rainfall events and year long accumulation in between R. M. Young rain gauges and ARGs; and seasonal agreement in between TRMM satellite data and ARGs.

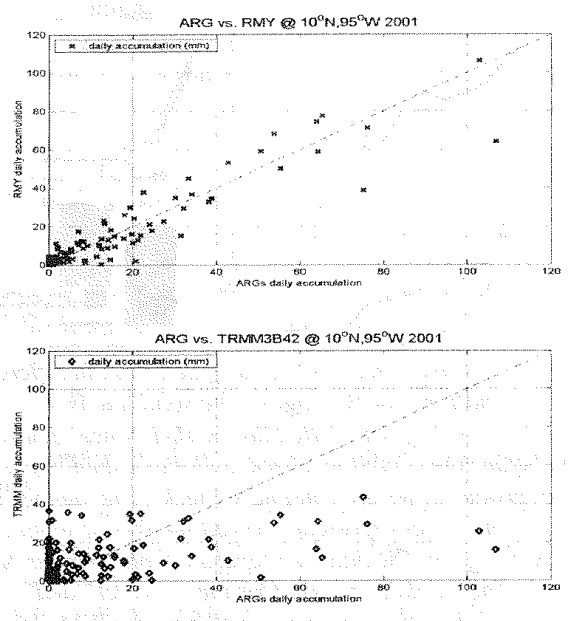

Fig. 8. The daily rainfall accumulation scatter plots. On the top panel, the ARG vs. R.M. Young rain gauge, shows good agreement in daily accumulation basis. The bottom panel is the ARG vs. TRMM Product 3B42.

Part of the acoustic rainfall measurement is objective detection of the rain. An acoustic discrimination method based on the frequency characteristics of the observed ambient sound spectrum and temporal reoccurrence is successful at retrieving the rainfall acoustic signals. The probability of false alarm is reduced to 0.4 % after the discrimination process. For rainfall rates over 15 mm/hr, acoustic detection is nearly 100 %.

The effect of wind on the acoustic signal from rain is examined and shown to be wind speed dependent. At lower frequencies, the signal from rainfall becomes "contaminated" by the sound produced from waves breaking. Contamination is frequency dependent and can be estimated. However, this separation may not be valid, especially at high rainfall rates and high wind speeds as the interaction of rain with the sound production mechanism for wind (breaking waves) is not fully understood. The unique spectral feature of light rain, a peak in the spectrum at 15-25 kHz is affected by wind. This spectral peak is due to the sound generated by small raindrops within the rain and is not a reliable indication of rainfall rate, but can be used to detect rainfall, even light drizzle. Above 30 kHz, the sound levels for high rainfall rates are observed to decrease as the wind speed increases. This is likely to be due to the attenuation of the rainfall signal by ambient bubbles that have been stirred down into the ocean and act as an absorption layer for an acoustic measurement made below the bubbles.

References:

Black, P. G., J. R. Proni, J. C. Wilkerson, and C. E. Samsury, 1997: Oceanic rainfall detection and

classification in tropical and subtropical mesoscale convective systems using underwater acoustic methods. *Mon. Wea. Rev.* **125**, 2014-2024.

Freitag, H.P., M. O'Haleck, G. C. Thomas, and M. J. McPhaden, 2001: Calibration procedures and instrumental accuracies for ATLAS wind measurements. *NOAA. Tech. Memo. OAR PMEL*-**119,** NOAA/Pacific Marine Environmental Laboratory, Seattle, Washington, 20 pp.

Ma, B. B., J. A. Nystuen, and R. C. Lien 2005: Prediction of underwater sound levels from rain and windThe Journal of the Acoustical Society of America, Vol. **117**, No. 6, pp. 3555–3565, June 2005

_____, and J. A. 2005: Passive Acoustic Detection and Measurement of Rainfall at Sea, *Journal of Atmospheric and Oceanic Technology*, Vol. 22, No. 8, pages 1225–1248.

Medwin, J. A. Nystuen, P. W. Jacobus, L. H. Ostwald, and D. E. Synder, 1992: The anatomy of underwater rain noise. *J. Acoust. Soc. Am.* **92**, 1613-1623.

Nystuen, J. A. 1993: An explanation of the sound generated by light rain in the presence of wind. *Natural Physical Sources of Underwater Sound*, B. R. Kerman, Ed., Kluwer Academic Publishers, 659-668.

_____, 1996: Acoustic rainfall analysis: Rainfall drop size distribution using the underwater sound field. *J. Atmos. And Oceanic Tech.*, **13**: 74-84.

_____, M. J. McPhaden, and H. P. Freitag, 2000: Surface measurements of precipitation from an ocean mooring: The Acoustic Log from the South China Sea. *J. Appl. Meteor.* **39**, 2182-2197.

_____, 2001: Listening to raindrops from underwater: An acoustic disdrometer. *J. Atmos. and Oceanic Tech.* **18**, 1640-1657.

Pumphrey, H. C., L. A. Crum, and L. Bjorno, 1989: Underwaer sound produced by individual drop impacts and rainfall. *J. Acoust. Soc. Amer.*, **85**, 1518-1526

Serra, Y., P. A. Hearn, H. P. Freitag, and M. J. McPhaden. 2001: ATLAS Self-siphoning rain gauge error estimates. *J.Atmos.and Oceanic Tech,*.**18**, 1989-2002

Urick, R. J., 1983: *Principles of Underwater Sound,* third ed. McGraw-Hill, 423 pp.

Vagle, S., W. G. Large, and D. M. Farmer. 1990: An evaluation of the WOTAN technique for inferring oceanic wind from underwater sound. *J. Atmos. and Ocean. Tech.* **7**, 576-595.